

Frequency Shift Observer for an SNS Superconducting RF Cavity

Sung-II Kwon, Amy Regan, and Mark Prokop

Abstract—In contrast to a normal conducting RF cavity, a superconducting RF cavity is very susceptible to shifts in its resonance frequency. The main sources of the shift are Lorentz force detuning and microphonics. In spallation neutron source, to compensate for the frequency shift, a feedforward control is to be applied. In this paper, as an initiative step, a frequency shift observer is proposed which is simple enough to be implemented with a digital signal processor in real time. Simulation results of the proposed frequency shift observer show reliable performance and acceptable computation time for the real time implementation.

Index Terms—Disturbance observer, feedback control, feedforward control, Lorentz force detuning, microphonics, spallation neutron source (SNS), superconducting RF cavity.

I. INTRODUCTION

THE spallation neutron source (SNS) linac to be built at Oak Ridge National Laboratory (ORNL), TN, consists of a combination of low energy normal conducting (NC) accelerating structures as well as higher energy superconducting RF (SRF) structures. In order to provide the stable cavity field so that the beam obtains the full power from the input RF power, the RF control systems for both the NC and SRF portions of the linac are designed to maintain the cavity field at a specific amplitude and phase.

In contrast to a NC cavity, an SRF cavity is very susceptible to the resonance frequency shift due to thin walls and high loaded Q . There are several sources of the resonance frequency shift, the major ones being the Lorentz force detuning and microphonics.

The RF magnetic field in a SRF cavity interacts with the RF wall current resulting in a Lorentz force, which is significant at high accelerating fields and for a pulsed accelerator such as an SNS or TESLA facility [1]. The radiation pressure, which is proportional to the square of magnetic field intensity and accelerating gradient, causes a small deformation of the cavity shape resulting in a shift of its resonance frequency, called Lorentz force detuning [2]. Lorentz force detuning influences the performance of the low level RF control system due to the extra power needed to control an incorrectly tuned cavity. In the feedback loop, a klystron can be treated as an actuator with nonlinear saturation characteristics. The klystron should not be operated in its saturation region. For the SNS SRF linac in SNS, RF power systems are designed to have 33% power control margin which is required to compensate for the Lorentz force detuning, micro-

phonics, transmission line losses, and electronic hardware disturbances. The required power due to the Lorentz force detuning is proportional to the square of the Lorentz force detuning. In the case of a medium beta SRF cavity #70 in the SNS SRF linac, the expected Lorentz force detuning is -307 Hz and the corresponding required power is 26 kW [3]. In order to prevent the klystron from operating in the saturation region, a hardware limiter or a software limiter can be implemented in the low level RF control system. In this case, when the low level RF control system output reaches the upper bound of the limiter due to the increasing Lorentz force detuning, the control system does not supply enough output to compensate for the Lorentz force detuning. One way to avoid this actuator saturation is to make the klystron operate in such a way that it generates enough maximum output power to guarantee power control margin for the frequency shift, thus requiring a lot of klystron power overhead for the minimum detuning regime. Another possible way is to apply predetuning (frequency offset). When the Lorentz force detuning due to one RF pulse decays rapidly enough to allow the initial values of the next RF pulse to be within a certain range, then the determination of the required predetuning is a relatively easy task. However, the initial values at the beginnings of RF pulses are difficult to predict [4].

Another source of the resonance frequency shift is microphonics [2]. The loaded Q , Q_L , of a SRF cavity is much higher than that of a NC cavity. The resulting narrow bandwidth makes SRF cavities more sensitive to mechanical vibrations. Heavy machinery can transmit mechanical vibrations through the beamline, ground, supports, and cryostat to the cavity. Mechanical vacuum pumps can interact with the cavity through the beam tubes. Vibrations generated by compressors and pumps of the refrigerator can be transmitted to the cavity. The spectrum of mechanical vibrations is filtered by the transfer medium and finally interacts with the cavity. In SNS, the expected microphonics amplitude limit is 100 Hz and the average value is 9 Hz [5].

The Lorentz force detuning can be compensated by increasing the mechanical stiffness of the cavity by using a mechanical structure such as stiffing ring and/or by applying a proper feedback or feedforward technique. In the TESLA facility, an adaptive feedforward control with piezosensor and piezoactuator (tuner), has been considered for RF pulse-to-pulse Lorentz force detuning compensation [6]. The control is based on experimental measurement of a SRF cavity after the cavity is assembled. Hence, the mechanical modes of interest are fixed and the Lorentz force detuning at the next RF pulse is predictable with the current measured data, that is, the Lorentz force detuning is highly repetitive. Also, with their cavity design, the Lorentz force detuning does not require excessive power control margin.

Manuscript received February 4, 2002; revised August 6, 2002.

The authors are with the SNS Division, Los Alamos National Laboratory, Los Alamos, NM 87545 USA (e-mail: skwon@lanl.gov).

Digital Object Identifier 10.1109/TNS.2002.807852

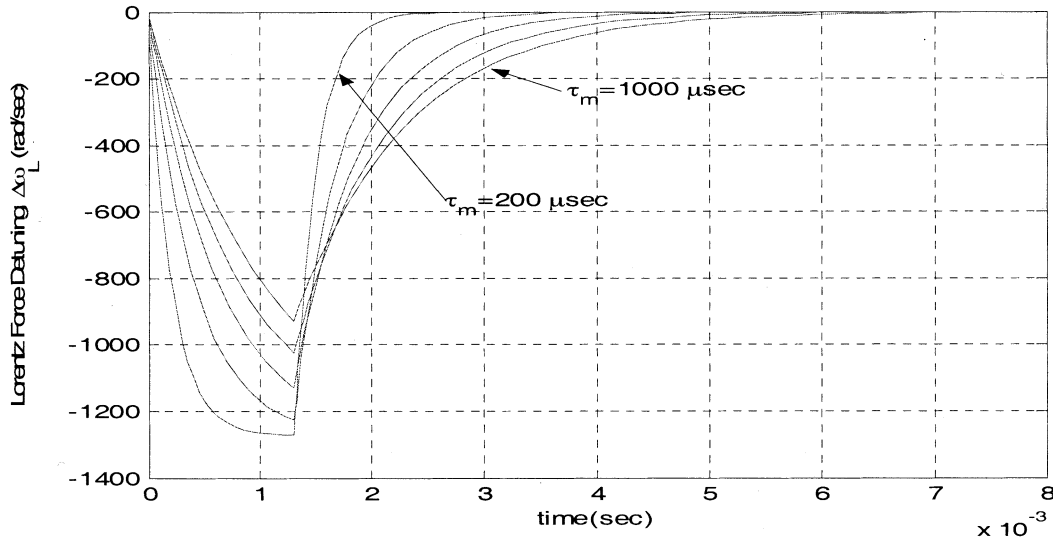


Fig. 1. Lorentz force detuning with respect to mechanical time constants.

In SNS, as an alternative approach, a pure feedforward control based on the disturbance estimation is considered. Compared with the case when the cavity is being driven on resonance, the frequency shift is a time varying disturbance and elimination of disturbance's effect is a major objective in the control of industrial systems. For linear systems, many approaches have been proposed to eliminate disturbance. The introduction of the integral action is an easily considered method. One way to embed the integral action is to enforce it in the controller as is the case of a PI controller. Another method is to model the disturbance and design a controller and then the integral action arises naturally. In [7] and [8], the Lorentz force detuning is modeled with a superposition of vibrations of mechanical modes in the SRF cavity and a proportional-integral derivative (PID) feedback controller used for the cavity field stabilization partially compensates for the Lorentz force detuning. When the variation rate of the disturbance is large or the magnitude of the Lorentz force detuning is large, then the performance of the controller where the integral action is embedded is not satisfactory. Specifically, when the magnitude of the Lorentz force detuning is large, then the RF pulse-to-pulse based feedforward control may not achieve the satisfactory performance. Before the feedforward control starts to work, the control system may lose its stability unless sufficient power control margin is reserved. Hence, it may be necessary to design a controller which is not based on RF pulse-to-pulse measurements but based on instantaneously measuring/estimating and updating data like Kalman prediction. When the Lorentz force detuning model considering all dominant mechanical mode frequencies is used, the controller complexity increases as well.

In order to incorporate the information on disturbances such as spectrum and magnitude to the controller, sensors are used to measure disturbances directly, or disturbance observers are designed and disturbance properties from the measured input-output data are estimated. In this paper, as an initiative step for a pure feedforward control, a frequency shift observer is proposed. The frequency shift observer yields the estimate of the frequency shift with measured outputs-cavity field in-phase

and quadrature, and measured inputs-klystron output in-phase and quadrature (or low level RF controller output in-phase and quadrature). The computational time of the frequency shift estimator is small enough to be implemented with a digital signal processor (DSP) in a real time manner. Based on the estimated frequency shift, a pure feedforward controller can be designed in such a way that the (time varying) tuning frequency (frequency offset), which is the negative of the estimated frequency shift, is generated.

II. LORENTZ FORCE DETUNING MODEL

The Lorentz force detuning is an important factor of the RF frequency shift in SRF cavities. Many researches have focused on the Lorentz force detuning modeling. The Lorentz force detuning is modeled as a first-order differential equation or as a second-order differential equation. When the damping is sufficiently large, then the second-order differential equation model is approximated by the first-order differential equation even though it is difficult to obtain large damping in a SRF cavity. With a feedback controller, the frequency shift can be compensated partially [7], [8]. However, there may be limitation to the performance achieved by the feedback controller. For SNS, the RF pulse repetition period is 16.667 ms (1/60 Hz). At the end of a RF pulse, the RF field constructed in a SRF cavity decays to zero with the cavity time constant much shorter than the time between RF pulses. Hence, the Lorentz force detuning during the RF pulse off period approximately behaves as a decaying oscillation, whose amplitude is determined by the values of the Lorentz force detuning and the variation rate of the Lorentz force detuning (velocity) at the end of the current RF pulse, and whose decay rate is determined by the damping constant of the mechanical mode.

A. First-Order State Space Model

The Lorentz force detuning is modeled as a first-order differential equation given below [1], [9]:

$$\dot{\omega}_L = -\frac{1}{\tau_m}\omega_L + \frac{2\pi}{\tau_m}k_{\text{LFD}}E_{\text{ACC}}^2 \quad (2.1)$$

where E_{ACC} is the accelerating gradient of a cavity and τ_m is the mechanical time constant of a cavity. The mechanical time constant determines whether the Lorentz force detuning decays completely or not at the instance of a new RF pulse. Fig. 1 shows the relation between the mechanical time constant and the Lorentz force detuning during one full RF repetition period (1/60 Hz) for $E_{\text{ACC}} = 10.07$ MV/m and for $K_{\text{LFD}} = -2.0$ Hz/(MV/m)². With the mechanical time constant, $\tau_m = 1.0$ msec, the decay time of the Lorentz force detuning is about 5.8 ms, which implies that there is no interaction between two consecutive RF pulses since the next RF pulse occurs 16.667 ms later.

The first-order state space model can be used for the approximation of the second-order model when the damping constant is sufficiently large. However, the numerical analysis [10], [11] show that the first-order state space model of the Lorentz force detuning is not appropriate due to small damping constants of the SNS SRF cavities.

B. Second-Order State Space Model

The situation is complicated when the Lorentz force detuning is modeled as a second-order differential equation and when several mechanical modes exist in a SRF cavity. Detailed investigation has been performed by Ellis [10] and Mitchell [11]. Sundelin [4] has investigated the Lorentz force detuning when the mechanical mode frequency is assumed to be 495 Hz with respect to mechanical quality factor, Q . For a medium- β SRF cavity in SNS, the cavity's mechanical damping constant is very small and so the developed Lorentz force detuning does not decay before the next RF pulse comes.

As was mentioned in [4], for the small damping constant, the swing of the developed Lorentz force detuning is 2 times that of the static Lorentz force detuning, i.e., $f_L = 2k_{\text{LFD}}E_{\text{ACC}}^2$. Hence, the power control margin estimation and the cavity field stabilization are much more complicated tasks. For a mechanical mode frequency, ω_{mi} , a second-order differential equation defines the Lorentz force detuning

$$\ddot{\omega}_L + a_1\dot{\omega}_L + \omega_{mi}^2\omega_L = bV^2 \quad (2.2)$$

where b is a weighting parameter to be specified in the following and

- ω_{mi}^2 (k/m);
- a_1 $2\zeta\omega_{mi}$
- m general mass;
- k stiffness constant;
- ζ damping constant;
- V cavity voltage.

Since the cavity voltage $V(t)$ and the accelerating electric field $E(t)$ are expressed as $V(t) = l \cdot E(t)$, l : cavity length, (2.2) can be written as

$$\ddot{\omega}_L + a_1\dot{\omega}_L + \omega_{mi}^2\omega_L = bl^2E^2(t). \quad (2.3)$$

The static Lorentz force detuning can be obtained by setting $\dot{\omega}_L = 0$ and $\ddot{\omega}_L = 0$ of (2.3)

$$\omega_{\text{LSS}} = \frac{bl^2}{\omega_{mi}^2}E_{\text{ACC}}^2. \quad (2.4)$$

Since the static Lorentz force detuning is given by

$$f_L = k_{\text{LFD}}E_{\text{ACC}}^2 \quad (2.5)$$

it follows from (2.4) and (2.5) that the constant b is given by

$$b = 2\pi k_{\text{LFD}} \frac{\omega_{mi}^2}{l^2}. \quad (2.6)$$

Inserting (2.6) to (2.3), we obtain

$$\ddot{\omega}_L + a_1\dot{\omega}_L + \omega_{mi}^2\omega_L = 2\pi k_{\text{LFD}}\omega_{mi}^2E^2(t). \quad (2.7)$$

Note that the first-order differential equation given in Section II-A is an approximation of the above equation in the case when the damping constant is sufficiently large.

Define

$$\begin{aligned} x_1 &= \omega_L, \\ x_2 &= \dot{\omega}_L = \dot{x}_1. \end{aligned}$$

Then, (2.7) can be written as the formal second-order state space equation describing the Lorentz force detuning due to a single mechanical mode vibration

$$\begin{bmatrix} \dot{x}_1 \\ \dot{x}_2 \end{bmatrix} = \begin{bmatrix} 0 & 1 \\ -\omega_{mi}^2 & -a_1 \end{bmatrix} \begin{bmatrix} x_1 \\ x_2 \end{bmatrix} + \begin{bmatrix} 0 \\ 2\pi k_{\text{LFD}}\omega_{mi}^2 \end{bmatrix} E^2(t) \quad (2.8)$$

$$y = [1 \quad 0] \begin{bmatrix} x_1 \\ x_2 \end{bmatrix}. \quad (2.9)$$

When multimechanical modes are considered, the modeling of the Lorentz force detuning is complicated. Cross coupling of mechanical mode vibrations must be considered. This means that the Lorentz force detuning constants $K_{\text{LFD}}^i, i = 1, 2, \dots, m$, for each mechanical mode are distributed with certain conditions, and boundary conditions of the second-order differential equations for each mechanical mode need to be assigned properly. Details are addressed in [8].

III. SUPERCONDUCTING RF CAVITY MODEL AND FREQUENCY SHIFT MODEL

A SRF cavity is given by the state space model [1], [12]

$$\dot{z} = A_z(\Delta\omega)z + B_z u + B_z I \quad (3.1)$$

$$y = C_z z \quad (3.2)$$

where

$$\begin{aligned} A_z(\Delta\omega) &= \begin{bmatrix} -\frac{1}{\tau_L} & -\Delta\omega \\ \Delta\omega & -\frac{1}{\tau_f} \end{bmatrix} \\ B_z &= \begin{bmatrix} \frac{2}{Z_o}c_1 & -\frac{2}{Z_o}c_3 \\ \frac{2}{Z_o}c_3 & \frac{2}{Z_o}c_1 \end{bmatrix} \\ B_z I &= \begin{bmatrix} -2c_1\zeta & 2c_3\zeta \\ -2c_3\zeta & -2c_1\zeta \end{bmatrix} \\ C_z &= \begin{bmatrix} 1 & 0 \\ 0 & 1 \end{bmatrix}, \quad z = \begin{bmatrix} z_1 \\ z_2 \end{bmatrix} = \begin{bmatrix} V_I \\ V_Q \end{bmatrix} \\ u &= \begin{bmatrix} u_1 \\ u_2 \end{bmatrix} = \begin{bmatrix} V_{fI} \\ V_{fQ} \end{bmatrix}, \quad I = \begin{bmatrix} I_I \\ I_Q \end{bmatrix} \end{aligned} \quad (3.3)$$

and

$$\begin{aligned} \Delta\omega &= \Delta\omega_B + \Delta\omega_L + \Delta\omega_{\text{MCP}} \\ c_1 &= \frac{R_{cu}}{\tau}, \quad c_3 = \frac{R_{cu}}{2Q_o\tau} \end{aligned} \quad (3.4)$$

and	
$\Delta\omega_B$	predetuning frequency against beam loading [rad/s];
$\Delta\omega_L$	Lorentz force detuning [rad/s];
$\Delta\omega_{MCP}$	microphonics [rad/s];
$\tau=(2Q_o/\omega_o)$	unloaded cavity damping time constant [s];
$\tau_L=(2Q_L/\omega_o)$	loaded cavity damping time constant [s];
Q_o	cavity resonator unloaded quality factor;
ω_o	cavity resonance frequency [rad/s];
R_{cu}	resistance of the Equivalent circuit of cavity transformed to RF generator [Ω];
Z_o	transmission line characteristic impedance [Ω];
ζ	transformation ratio;
V_{fI}, V_{fQ}	forward In-phase (I) and quadrature (Q) [V];
I_I, I_Q	beam current in In-phase (I) and quadrature (Q) [A];
V_I, V_Q	cavity field in-phase (I) and quadrature (Q) [V].

Note that since $Q_o \approx 10^9 \sim 10^{10}$, $c_3 \approx 0$. In the above model, $\Delta\omega$ is the sum of the predetuning, $\Delta\omega_B$, the Lorentz force detuning, $\Delta\omega_L$, and microphonics, $\Delta\omega_{MCP}$. The state space model given by (3.1)–(3.2) can be written by

$$\dot{z} = A_{zo}z + B_z u + B_{zI} I + \begin{bmatrix} -\Delta\omega y_2 \\ \Delta\omega y_1 \end{bmatrix} \quad (3.5)$$

$$y = C_z z \quad (3.6)$$

where

$$A_{zo} = \begin{bmatrix} -\frac{1}{\tau_L} & 0 \\ 0 & -\frac{1}{\tau_L} \end{bmatrix}. \quad (3.7)$$

The objective of this paper is to design an observer such that the estimate $\Delta\hat{\omega}$ yielded by the observer exponentially approaches the frequency shift $\Delta\omega$. As mentioned in the previous section, when the Lorentz force detuning model includes all mechanical mode dynamics, the observer structure may be complicated and computational complexity increases. Instead of this complex higher order model, the frequency shift is modeled as

$$\Delta\dot{\omega} = 0. \quad (3.8)$$

The model (3.8) is widely used for constant or slowly varying disturbance. The augmented state space model is with outputs, y_1, y_2 and inputs u_1, u_2

$$\begin{aligned} \begin{bmatrix} \dot{z}_1 \\ \dot{z}_2 \\ \Delta\dot{\omega} \end{bmatrix} &= \begin{bmatrix} 0 & 0 & -y_2 \\ 0 & 0 & y_1 \\ 0 & 0 & 0 \end{bmatrix} \begin{bmatrix} z_1 \\ z_2 \\ \Delta\omega \end{bmatrix} \\ &+ \begin{bmatrix} -\frac{1}{\tau_L} & 0 \\ 0 & -\frac{1}{\tau_L} \\ 0 & 0 \end{bmatrix} \begin{bmatrix} y_1 \\ y_2 \end{bmatrix} \\ &+ \begin{bmatrix} \frac{2}{Z_o} c_1 & -\frac{2}{Z_o} c_3 \\ \frac{2}{Z_o} c_3 & \frac{2}{Z_o} c_1 \end{bmatrix} \begin{bmatrix} u_1 \\ u_2 \end{bmatrix} + \begin{bmatrix} B_{zI} \\ 0 \end{bmatrix} I \quad (3.9) \end{aligned}$$

$$y = \begin{bmatrix} C_z & 0 \end{bmatrix} \begin{bmatrix} z_1 \\ z_2 \\ \Delta\omega \end{bmatrix}. \quad (3.10)$$

IV. FREQUENCY SHIFT OBSERVERS

A. First-Order State Space Model

The frequency shift is modeled as given in (3.8) If an observer has sufficiently fast dynamics as compared with the time variations of the Lorentz force detuning and microphonics, the observer can estimate the frequency shift due to the Lorentz force detuning, microphonics, and predetuning against beam loading. For the augmented system given by (3.9)–(3.10), a full-order observer is proposed [13]

$$\begin{aligned} \begin{bmatrix} \dot{\hat{z}}_1 \\ \dot{\hat{z}}_2 \\ \Delta\dot{\hat{\omega}} \end{bmatrix} &= \begin{bmatrix} 0 & 0 & -y_2 \\ 0 & 0 & y_1 \\ 0 & 0 & 0 \end{bmatrix} \begin{bmatrix} \hat{z}_1 \\ \hat{z}_2 \\ \Delta\hat{\omega} \end{bmatrix} + \begin{bmatrix} -\frac{1}{\tau_L} & 0 \\ 0 & -\frac{1}{\tau_L} \\ 0 & 0 \end{bmatrix} \begin{bmatrix} y_1 \\ y_2 \end{bmatrix} \\ &+ \begin{bmatrix} \frac{2}{Z_o} c_1 & -\frac{2}{Z_o} c_3 \\ \frac{2}{Z_o} c_3 & \frac{2}{Z_o} c_1 \end{bmatrix} \begin{bmatrix} u_1 \\ u_2 \end{bmatrix} \\ &+ \begin{bmatrix} \frac{2}{Z_o} c_1 & -\frac{2}{Z_o} c_3 \\ \frac{2}{Z_o} c_3 & \frac{2}{Z_o} c_1 \end{bmatrix} \begin{bmatrix} u_1 \\ u_2 \end{bmatrix} \\ &+ K_{fob}(y_1, y_2, u_1, u_2) \left(\begin{bmatrix} y_1 \\ y_2 \end{bmatrix} - \begin{bmatrix} C_z & 0 \end{bmatrix} \begin{bmatrix} \hat{z}_1 \\ \hat{z}_2 \\ \Delta\hat{\omega} \end{bmatrix} \right) \quad (4.1) \end{aligned}$$

where $K_{fob}(y_1, y_2, u_1, u_2)$ is a nonlinear observer gain matrix.

Define the observer error as

$$\hat{e} = \begin{bmatrix} z_1 \\ z_2 \\ \Delta\omega \end{bmatrix} - \begin{bmatrix} \hat{z}_1 \\ \hat{z}_2 \\ \Delta\hat{\omega} \end{bmatrix}. \quad (4.2)$$

The observer error dynamics is given by

$$\begin{aligned} \dot{\hat{e}} &= \begin{bmatrix} 0 & 0 & -y_2 \\ 0 & 0 & y_1 \\ 0 & 0 & 0 \end{bmatrix} \hat{e} - K_{fob}(y_1, y_2, u_1, u_2) \\ &\times \left(\begin{bmatrix} y_1 \\ y_2 \end{bmatrix} - \begin{bmatrix} C_z & 0 \end{bmatrix} \begin{bmatrix} \hat{z}_1 \\ \hat{z}_2 \\ \Delta\hat{\omega} \end{bmatrix} \right) + \begin{bmatrix} B_{zI} \\ 0 \end{bmatrix} I \\ &= \begin{bmatrix} 0 & 0 & -y_2 \\ 0 & 0 & y_1 \\ 0 & 0 & 0 \end{bmatrix} \hat{e} - K_{fob}(y_1, y_2, u_1, u_2) \\ &\times \begin{bmatrix} C_z & 0 \end{bmatrix} \hat{e} + \begin{bmatrix} B_{zI} \\ 0 \end{bmatrix} I \\ &= \begin{bmatrix} 0 & 0 & -y_2 \\ 0 & 0 & y_1 \\ 0 & 0 & 0 \end{bmatrix} - K_{fob}(y_1, y_2, u_1, u_2) \begin{bmatrix} C_z & 0 \end{bmatrix} \hat{e} \\ &+ \begin{bmatrix} B_{zI} \\ 0 \end{bmatrix} I \\ &\equiv A_{fob} \hat{e} + \begin{bmatrix} B_{zI} \\ 0 \end{bmatrix} I. \quad (4.3) \end{aligned}$$

The gain matrix $K_{\text{fob}}(y_1, y_2, u_1, u_2)$ is designed so that the matrix A_{fob} is Hurwitz stable. The assignability of the poles of A_{fob} is given by the (local) observability at y_1, y_2 which is characterized by the observability matrix [13], [14]

$$W_{\text{obsv}}(y_1, y_2) = \begin{bmatrix} I_{2 \times 2} & 0_{2 \times 1} \\ 0_{2 \times 2} & \begin{bmatrix} y_1 \\ y_2 \end{bmatrix} \\ 0 & 0 \\ \vdots & \vdots \\ 0 & 0 \end{bmatrix}. \quad (4.4)$$

Whenever $W_{\text{obsv}}(y_1, y_2)$ has full rank at y_1, y_2 , then the augmented system is locally observable. Since $\text{rank}(W_{\text{obsv}}(y_1, y_2)) = 2 + 1 = 3$, the augmented system is observable and the poles of A_{fob} can be assigned arbitrarily.

When beam is not loaded ($I = 0$), the observer error dynamics (4.3) is reduced to

$$\dot{\hat{e}} = A_{\text{fob}} \hat{e}.$$

Hence, the estimate error converges to zero and $\Delta\hat{\omega}$ is the estimate of the lumped sum, $\Delta\omega_B + \Delta\omega_L + \Delta\omega_{\text{MCP}}$. When beam is loaded ($I \neq 0$), since the frequency shift due to beam loading is asymptotically cancelled out by the predetuning, $\Delta\omega_B$, the observer error dynamics (4.3) asymptotically approaches to

$$\dot{\hat{e}} = A_{\text{fob}} \hat{e}$$

and the estimate error converges to zero and $\Delta\hat{\omega}$ is the estimate of the lumped sum, $\Delta\omega_L + \Delta\omega_{\text{MCP}}$.

B. Reduced-Order Observer

The full-order observer uses all state variables of the augmented system and as a result the observer has the dimension 3. It is possible to build a reduced order observer if the number of the state variables of the original system, 2 is strictly greater than the number of the disturbance $\Delta\omega$ to be estimated 1. The minimal order possible is 2 ($= 2 \cdot 1$).

Define the augmented state vector as

$$v = \begin{bmatrix} z_2 \\ \Delta\omega \end{bmatrix}. \quad (4.5)$$

The reduced augmented system is given by

$$\begin{aligned} \begin{bmatrix} \dot{z}_2 \\ \Delta\dot{\omega} \end{bmatrix} &= \begin{bmatrix} 0 & y_1 \\ 0 & 0 \end{bmatrix} \begin{bmatrix} z_2 \\ \Delta\omega \end{bmatrix} + \begin{bmatrix} 0 & -\frac{1}{\tau_L} \\ 0 & 0 \end{bmatrix} \begin{bmatrix} y_1 \\ y_2 \end{bmatrix} \\ &+ \begin{bmatrix} \frac{2}{Z_o} c_3 & \frac{2}{Z_o} c_1 \\ 0 & 0 \end{bmatrix} \begin{bmatrix} u_1 \\ u_2 \end{bmatrix} \\ &+ \begin{bmatrix} -2c_3\varsigma & -2c_1\varsigma \\ 0 & 0 \end{bmatrix} \begin{bmatrix} I_I \\ I_Q \end{bmatrix} \end{aligned} \quad (4.6)$$

$$\bar{y} = \bar{C} \begin{bmatrix} z_2 \\ \Delta\omega \end{bmatrix} = [1 \quad 0] \begin{bmatrix} z_2 \\ \Delta\omega \end{bmatrix}. \quad (4.7)$$

Define a reduced order observer as follows:

$$\begin{aligned} \begin{bmatrix} \dot{\hat{z}}_2 \\ \Delta\hat{\omega} \end{bmatrix} &= \begin{bmatrix} 0 & y_1 \\ 0 & 0 \end{bmatrix} \begin{bmatrix} \hat{z}_2 \\ \Delta\hat{\omega} \end{bmatrix} + \begin{bmatrix} 0 & -\frac{1}{\tau_L} \\ 0 & 0 \end{bmatrix} \begin{bmatrix} y_1 \\ y_2 \end{bmatrix} \\ &+ \begin{bmatrix} \frac{2}{Z_o} c_3 & \frac{2}{Z_o} c_1 \\ 0 & 0 \end{bmatrix} \begin{bmatrix} u_1 \\ u_2 \end{bmatrix} \\ &+ K_{\text{rob}}(y_1, y_2, u_1, u_2) \left(\bar{y} - \bar{C} \begin{bmatrix} \hat{z}_2 \\ \Delta\hat{\omega} \end{bmatrix} \right) \end{aligned} \quad (4.8)$$

where

$$K_{\text{rob}}(y_1, y_2, u_1, u_2) = \begin{bmatrix} K_{1\text{rob}}(y_1, y_2, u_1, u_2) \\ K_{2\text{rob}}(y_1, y_2, u_1, u_2) \end{bmatrix}. \quad (4.9)$$

Define the estimate error as

$$\hat{e} = \begin{bmatrix} z_2 \\ \Delta\omega \end{bmatrix} - \begin{bmatrix} \hat{z}_2 \\ \Delta\hat{\omega} \end{bmatrix}. \quad (4.10)$$

Then, the estimate error dynamics is given by

$$\begin{aligned} \dot{\hat{e}} &= \begin{bmatrix} 0 & y_1 \\ 0 & 0 \end{bmatrix} \hat{e} - K_{\text{rob}}(y_1, y_2, u_1, u_2) \left(\bar{y} - \bar{C} \begin{bmatrix} \hat{z}_2 \\ \Delta\hat{\omega} \end{bmatrix} \right) \\ &+ \begin{bmatrix} -2c_3\varsigma & -2c_1\varsigma \\ 0 & 0 \end{bmatrix} \begin{bmatrix} I_I \\ I_Q \end{bmatrix} \\ &= \begin{bmatrix} 0 & y_1 \\ 0 & 0 \end{bmatrix} \hat{e} - K_{\text{rob}}(y_1, y_2, u_1, u_2) \bar{C} \hat{e} \\ &+ \begin{bmatrix} -2c_3\varsigma & -2c_1\varsigma \\ 0 & 0 \end{bmatrix} \begin{bmatrix} I_I \\ I_Q \end{bmatrix} \\ &= \left[\begin{bmatrix} 0 & y_1 \\ 0 & 0 \end{bmatrix} - K_{\text{rob}}(y_1, y_2, u_1, u_2) \bar{C} \right] \hat{e} \\ &+ \begin{bmatrix} -2c_3\varsigma & -2c_1\varsigma \\ 0 & 0 \end{bmatrix} \begin{bmatrix} I_I \\ I_Q \end{bmatrix} \\ &\equiv A_{\text{rob}} \hat{e} + \begin{bmatrix} -2c_3\varsigma & -2c_1\varsigma \\ 0 & 0 \end{bmatrix} \begin{bmatrix} I_I \\ I_Q \end{bmatrix}. \end{aligned} \quad (4.11)$$

Since the reduced augmented system is locally observable, the poles of the matrix A_{rob} are arbitrarily assignable. Let r_1 and r_2 be stable desired poles of A_{rob} . Since

$$\begin{aligned} &\left| sI - \left[\begin{bmatrix} 0 & y_1 \\ 0 & 0 \end{bmatrix} - K_{\text{rob}}(y_1, y_2, u_1, u_2) \bar{C} \right] \right| \\ &= s^2 + K_{1\text{rob}}(y_1, y_2, u_1, u_2)s + K_{2\text{rob}}(y_1, y_2, u_1, u_2)y_1 \end{aligned} \quad (4.12)$$

the observer gains are given by

$$K_{1\text{rob}}(y_1, y_2, u_1, u_2) = -(r_1 + r_2) \quad (4.13)$$

$$K_{2\text{rob}}(y_1, y_2, u_1, u_2) = \frac{r_1 r_2}{y_1}. \quad (4.14)$$

By choosing r_1 and r_2 properly, the speed of the observation is determined.

When beam is not loaded ($I = 0$), the observer error dynamics (4.11) is reduced to

$$\dot{\hat{e}} = A_{\text{rob}} \hat{e}.$$

Hence, the estimate error converges to zero and $\Delta\hat{\omega}$ is the estimate of the lumped sum, $\Delta\omega_B + \Delta\omega_L + \Delta\omega_{\text{MCP}}$. When beam is loaded ($I \neq 0$), since the frequency shift due to beam loading is asymptotically cancelled out by the predetuning, $\Delta\omega_B$, the observer error dynamics (4.11) asymptotically approaches to

$$\dot{\hat{e}} = A_{\text{rob}} \hat{e}$$

and the estimate error converges to zero and $\Delta\hat{\omega}$ is the estimate of the lumped sum, $\Delta\omega_L + \Delta\omega_{\text{MCP}}$.

C. Nonlinear First-Order Observer

The reduced observer given by (4.8) estimates both the state z_2 and the frequency shift $\Delta\omega$. However, the state z_2 is the output y_2 and, hence, it is unnecessary to include the estimate \hat{z}_2 in the observer. In this section, a pure disturbance observer, frequency shift observer, is proposed.

Consider the state equation for the cavity field quadrature (Q)

$$\dot{z}_2 = y_1 \Delta\omega - \frac{1}{\tau_L} z_2 + \frac{2}{Z_o} c_3 u_1 + \frac{2}{Z_o} c_1 u_2 - 2c_3\varsigma I_I - 2c_1\varsigma I_Q. \quad (4.15)$$

Equation (4.15) is written as

$$y_1 \Delta\omega = \dot{z}_2 + \frac{1}{\tau_L} z_2 - \frac{2}{Z_o} c_3 u_1 - \frac{2}{Z_o} c_1 u_2 + 2c_3 \zeta I_I + 2c_1 \zeta I_Q. \quad (4.16)$$

Consider the term $2c_3 \zeta I_I + 2c_1 \zeta I_Q$ of the right-hand side of (4.16). It follows that

$$\begin{aligned} & 2c_3 \zeta I_I + 2c_1 \zeta I_Q \\ &= 2 \frac{R_{cu}}{2\tau Q_o} \frac{V_c}{V_f} I_b \cos(\phi_s) + 2 \frac{R_{cu}}{\tau} \frac{V_c}{V_f} I_b \sin(\phi_s) \\ &= 2 \frac{\omega_o}{2Q_o} \frac{1}{2Q_o} \frac{V_f^2}{2P_{cu}} \frac{V_c}{V_f} I_b \cos(\phi_s) \\ &\quad + 2 \frac{\omega_o}{2Q_o} \frac{V_f^2}{2P_{cu}} \frac{V_c}{V_f} I_b \sin(\phi_s) \\ &= \frac{\omega_o}{2Q_o} \frac{1}{2Q_o} \frac{V_c}{P_{cu}} I_b \cos(\phi_s) V_f + \frac{\omega_o}{2Q_o} \frac{V_c}{P_{cu}} I_b \sin(\phi_s) V_f \\ &= \frac{\omega_o}{2Q_o} \frac{1}{2Q_o} \frac{P_b}{P_{cu}} V_f + \frac{\omega_o}{2Q_o} \frac{P_b}{P_{cu}} \tan(\phi_s) V_f \\ &= \frac{\omega_o}{2Q_o} \frac{P_b}{P_{cu}} \left(\frac{1}{2Q_o} + \tan(\phi_s) \right) V_f \end{aligned} \quad (4.17)$$

where V_f is the forward voltage desired for the cavity field amplitude, P_{cu} is the wall power dissipation, P_b is the beam power, V_c is the design cavity voltage, and ϕ_s is the synchronous phase. Since $Q_o \gg 1$ and $(P_b/P_{cu}) \approx \beta$ for a SRF cavity, (4.17) reduces to

$$2c_3 \zeta I_I + 2c_1 \zeta I_Q = \frac{\omega_o}{2Q_L} \tan(\phi_s) V_f. \quad (4.18)$$

Consider the predetuning frequency $\Delta\omega_B$. Since

$$\tan(\psi) = 2Q_L \frac{\Delta\omega_B}{\omega_o} \quad (4.19)$$

where ψ is the detuning angle due to the beam loading and since the beam loading factor $\beta \gg 1$ for a SRF cavity, it is given by

$$\tan(\psi) = \frac{\beta - 1}{\beta + 1} \tan(\phi_s) \approx \tan(\phi_s). \quad (4.20)$$

It follows from (4.19) and (4.20) that

$$y_1 \Delta\omega_B = y_1 \frac{\omega_o}{2Q_L} \tan(\phi_s). \quad (4.21)$$

Now consider (4.18) and (4.21). When the cavity operates on resonance with a generator and the cavity field is settled down to the neighborhood of the desired values, then the imaginary part of the cavity field, y_2 , is close to zero, which yields $V_f \approx \sqrt{y_1^2 + y_2^2} \approx y_1$. Therefore,

$$y_1 \Delta\omega_B \approx 2c_3 \zeta I_I + 2c_1 \zeta I_Q \quad (4.22)$$

and (4.16) can be written as

$$y_1 \Delta\omega = \dot{z}_2 + \frac{1}{\tau_L} z_2 - \frac{2}{Z_o} c_3 u_1 - \frac{2}{Z_o} c_1 u_2$$

where $\Delta\omega = \Delta\omega_L + \Delta\omega_{MCP}$.

In summary, it follows from (3.4) and (4.22) that (4.16) has two forms depending upon whether beam is loaded or not. When beam is unloaded, (4.16) reduces to

$$\begin{aligned} y_1 \Delta\omega &= \dot{z}_2 + \frac{1}{\tau_L} z_2 - \frac{2}{Z_o} c_3 u_1 - \frac{2}{Z_o} c_1 u_2 \\ \Delta\omega &= \Delta\omega_B + \Delta\omega_L + \Delta\omega_{MCP} \end{aligned} \quad (4.23)$$

and when beam is loaded, it reduces to

$$\begin{aligned} y_1 \Delta\omega &= \dot{z}_2 + \frac{1}{\tau_L} z_2 - \frac{2}{Z_o} c_3 u_1 - \frac{2}{Z_o} c_1 u_2 \\ \Delta\omega &= \Delta\omega_L + \Delta\omega_{MCP}. \end{aligned} \quad (4.24)$$

For the frequency shift estimation, a disturbance observer is proposed as follows:

$$\Delta\hat{\omega} = -Ly_1 \Delta\hat{\omega} + L \left(\dot{z}_2 + \frac{1}{\tau_L} z_2 - \frac{2}{Z_o} c_3 u_1 - \frac{2}{Z_o} c_1 u_2 \right). \quad (4.25)$$

It follows from (3.8) and (4.25) that the observer error dynamics is given by

$$\begin{aligned} \dot{e} &= \Delta\dot{\omega} - \Delta\dot{\hat{\omega}} \\ &= Ly_1 \Delta\hat{\omega} - L \left(\dot{z}_2 + \frac{1}{\tau_L} z_2 - \frac{2}{Z_o} c_3 u_1 - \frac{2}{Z_o} c_1 u_2 \right) \\ &= Ly_1 \Delta\hat{\omega} - Ly_1 \Delta\omega \\ &= -Ly_1 e. \end{aligned} \quad (4.26)$$

The observer gain L is determined so that the characteristic equation

$$s + Ly_1 = 0 \quad (4.27)$$

has a desired root in the left half plane of the complex domain. The observer error dynamics (4.26) shows that for a properly chosen gain L , the estimate $\Delta\hat{\omega}$ asymptotically converges to $\Delta\omega_B + \Delta\omega_L + \Delta\omega_{MCP}$ when beam is unloaded, and to $\Delta\omega_L + \Delta\omega_{MCP}$ when beam is loaded.

The observer (4.25) is difficult to implement practically because the derivative term \dot{z}_2 is noisy and is hard to measure. A filter whose transfer function is $(s/\varepsilon s + 1)$ where ε is a small constant can be used to approximate the derivative. In this paper, a new variable is introduced

$$\hat{g}_L = \Delta\hat{\omega} - p(z_2) \quad (4.28)$$

where $p(z_2)$ is a nonlinear function of z_2 to be determined as follows.

The derivative of (4.28) with respect to time is

$$\begin{aligned} \dot{\hat{g}}_L &= \Delta\dot{\hat{\omega}} - \frac{\partial p(z_2)}{\partial z_2} \frac{dz_2}{dt} \\ &= -Ly_1 \Delta\hat{\omega} + L \left(\dot{z}_2 + \frac{1}{\tau_L} z_2 - \frac{2}{Z_o} c_3 u_1 - \frac{2}{Z_o} c_1 u_2 \right) - \frac{\partial p(z_2)}{\partial z_2} \dot{z}_2 \\ &= -Ly_1 \hat{g}_L + L \left(\dot{z}_2 + \frac{1}{\tau_L} z_2 - \frac{2}{Z_o} c_3 u_1 - \frac{2}{Z_o} c_1 u_2 - y_1 p(z_2) \right) - \frac{\partial p(z_2)}{\partial z_2} \dot{z}_2. \end{aligned} \quad (4.29)$$

When $p(z_2)$ is determined so that it satisfies

$$\frac{\partial p(z_2)}{\partial z_2} = L \quad (4.30)$$

then (4.29) reduces to

$$\dot{\hat{g}}_L = -Ly_1 \hat{g}_L + L \left(\frac{1}{\tau_L} z_2 - \frac{2}{Z_o} c_3 u_1 - \frac{2}{Z_o} c_1 u_2 - y_1 p(z_2) \right) \quad (4.31)$$

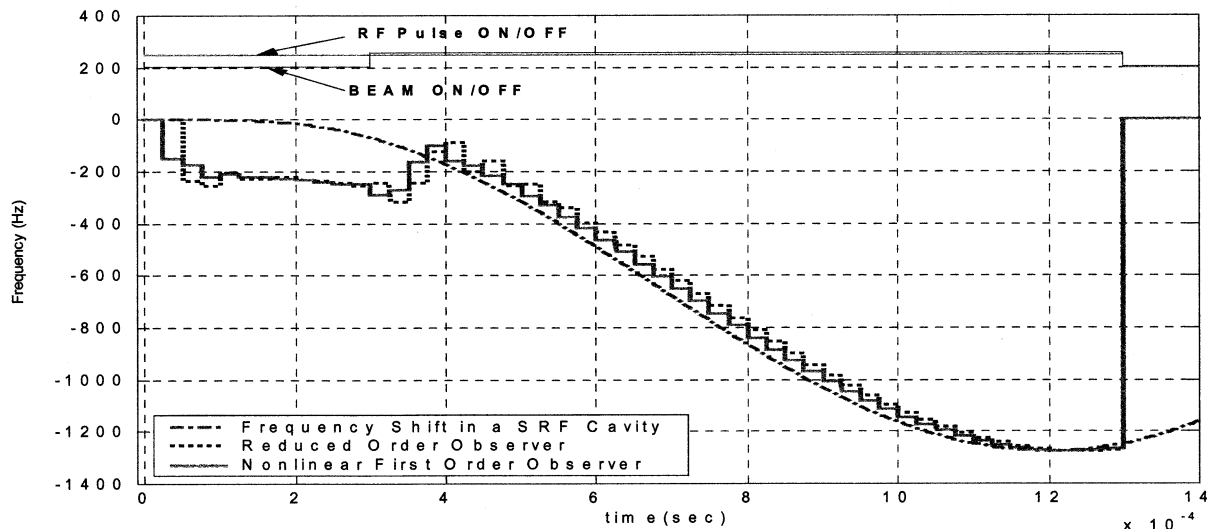


Fig. 2. Observer performances for the Lorentz force detuning in [3]. For the reduced observer, $r_1 = r_2 = 6.2832e4$ are used and for the nonlinear first-order observer, $l = 6.2834e4$ is used. Microphonics is not included in the model.

and the Lorentz force detuning estimate is given by

$$\Delta\hat{\omega} = \hat{g}_L + p(z_2). \quad (4.32)$$

It is easily verified that the observer error dynamics is given by

$$\dot{e} = \Delta\dot{\omega} - \Delta\dot{\hat{\omega}} = -\dot{g}_L - \frac{\partial p(z_2)}{\partial z_2} \frac{dz_2}{dt} = -Ly_1e. \quad (4.33)$$

The estimate $\Delta\hat{\omega}$ approaches the frequency shift $\Delta\omega$ if L is chosen such that (4.33) is asymptotically stable. One possible solution for L is

$$L = \frac{l}{y_1} \quad (4.34)$$

where l is a positive constant. In this case, the observer error dynamics becomes

$$\dot{e} + le = 0 \quad (4.35)$$

and the convergence rate can be specified by the parameter l . From (4.30), the corresponding $p(z_2)$ becomes

$$p(z_2) = \frac{l}{y_1} z_2. \quad (4.36)$$

V. SIMULATIONS AND EXPERIMENTS

In the previous section, three frequency shift observers have been proposed. For SNS, an observer is to be used together with the piezoactuator in order to compensate for the frequency shift in a SRF cavity. The chosen observer is implemented with a DSP and so the observer should be as simple as possible for the real time implementation provided with satisfactory performance. In addition, the observer is turned on when the RF is turned on and is turned off when RF is turned off. During the RF turn off period, the cavity field control is turned off and hence, the in-phase and quadrature of cavity field are difficult to predict. If their behaviors during the RF off period are the solutions of the stable first-order differential equations with zero inputs, then the pro-

posed observer do not need to be turned off and it can estimate frequency shift. As mentioned in [10], the dominant frequencies of the mechanical modes for the medium- β SRF section exist up to 2.0 kHz and the dominant frequencies of microphonics are within a few hundred Hertz. For satisfactory performance of the observer, the sampling frequency of the observer must be at least 20 kHz. The simple Euler method is used for the discretization of the observers and the reduced observer and the nonlinear first-order observer are simulated in the MATLAB/SIMULINK [15] environment.

Fig. 2 shows the observer performances where the Lorentz force detuning of a single mechanical mode of frequency 494.73 Hz [4], predetuning against beam loading, and beam loading yield frequency shift. Fig. 2 illustrates that the nonlinear first-order observer yields better performance over the reduced order observer. The sampling frequency of both observers is 40 kHz. Note that in Fig. 2, during the cavity filling time (RF pulse ON, beam OFF), the sum of the Lorentz force detuning and the predetuning against beam loading, $\Delta f_B = (f_0/2Q_L)(\beta - 1/\beta + 1) \tan \phi_s = -222.5$ Hz, is estimated. During the beam loading period (RF pulse ON, beam ON), the predetuning frequency is cancelled out by beam loading and the observers estimate the Lorentz force detuning. Fig. 3 shows the simulation results where microphonics is additionally included in the model. During the cavity filling time (RF pulse ON, beam OFF), the sum of the Lorentz force detuning, microphonics, and the predetuning against beam loading, is estimated. During the beam loading period (RF pulse ON, beam ON), the predetuning is offset by beam loading and the observers estimate the sum of the Lorentz force detuning and microphonics. Fig. 4 shows the simulation results where the Lorentz force detuning as addressed in [10] is considered. In this simulation, microphonics is not included.

The discretized observers are sensitive to both the observer gains and the sampling frequency. For a fixed sampling frequency of 40 kHz, in order to investigate the observer perfor-

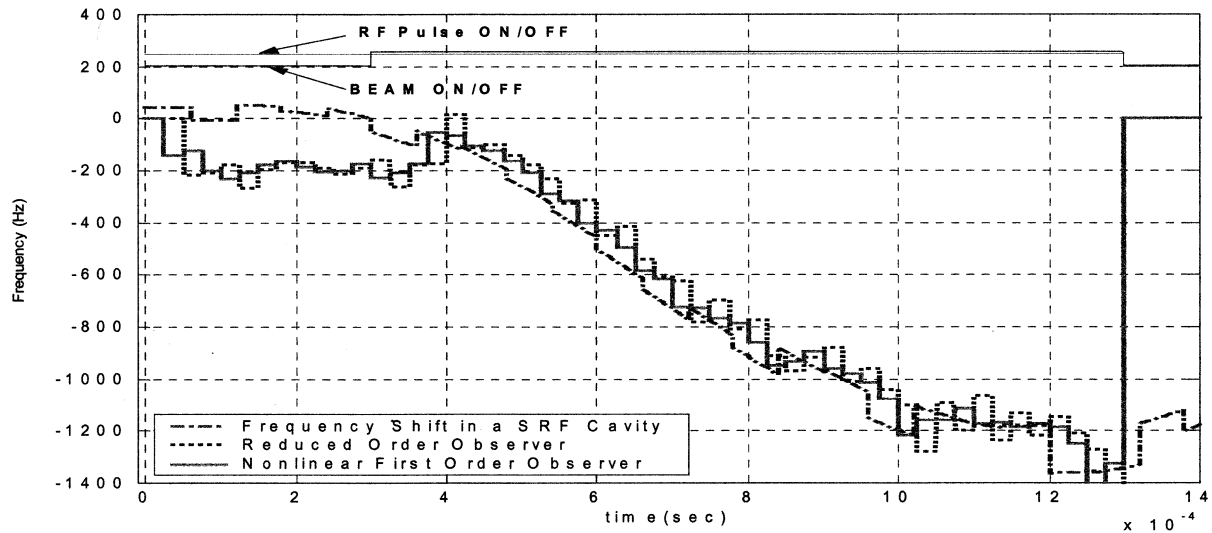


Fig. 3. Observer performances for the Lorentz force detuning in [3]. For the reduced observer, $r_1 = r_2 = 6.2832e4$ are used and for the nonlinear first-order observer, $l = 6.2834e4$ is used. Microphonics is included in the model.

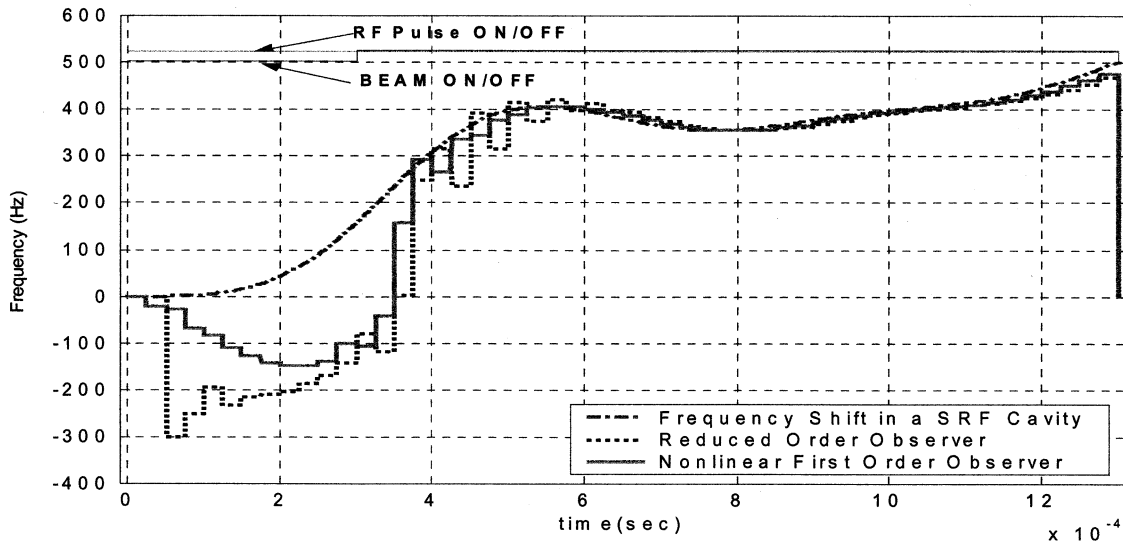


Fig. 4. Observer performances for the Lorentz force detuning in [8]. For the reduced observer, $r_1 = r_2 = 6.2832e4$ are used and for the nonlinear first-order observer, $l = 6.2834e4$ is used. Microphonics is not included in the model.

manances with respect to observer gains, different r_1, r_2 and l are applied. Fig. 5 shows this simulation results, which illustrate that the reduced order observer is more sensitive to the observer gain change than the nonlinear first-order observer. When the sampling frequency is increased, higher observer gains can be used and observers guarantee fast responses with initial fast decaying oscillation.

Considering the simulation results, the nonlinear first-order observer is chosen for the frequency shift observer of a SRF cavity. The observer is implemented in a TMS320C6201 evaluation module (EVM) [16], which includes an A/D converter (ADC) and a D/A converter (DAC). The clock speed of the DSP is 133 MHz and the sampling frequency of the ADC and DAC is 40 kHz. Currently, a prototype SRF cavity is being developed at

Jefferson National Laboratory, so real data is not yet available. At Los Alamos National Laboratory, extensive modeling and simulation with MATLAB/SIMULINK for a SRF cavity has been performed [17]. For the observer performance investigation, SIMULINK simulation data of the klystron output I/Q and cavity field I/Q were used and the observer was implemented in a TMS 320C6201 EVM.

Fig. 6 shows the experiment result of the nonlinear first-order observer where the Lorentz force detuning results from a 494.73-Hz-single-mechanical-mode vibration [4]. Fig. 7 shows the result of the nonlinear first-order observer where the Lorentz force detuning results from 29 mechanical mode vibrations [10]. For one data sample, the computational time was 21 CPU clock cycles. When 200 MHz CPU clock is used

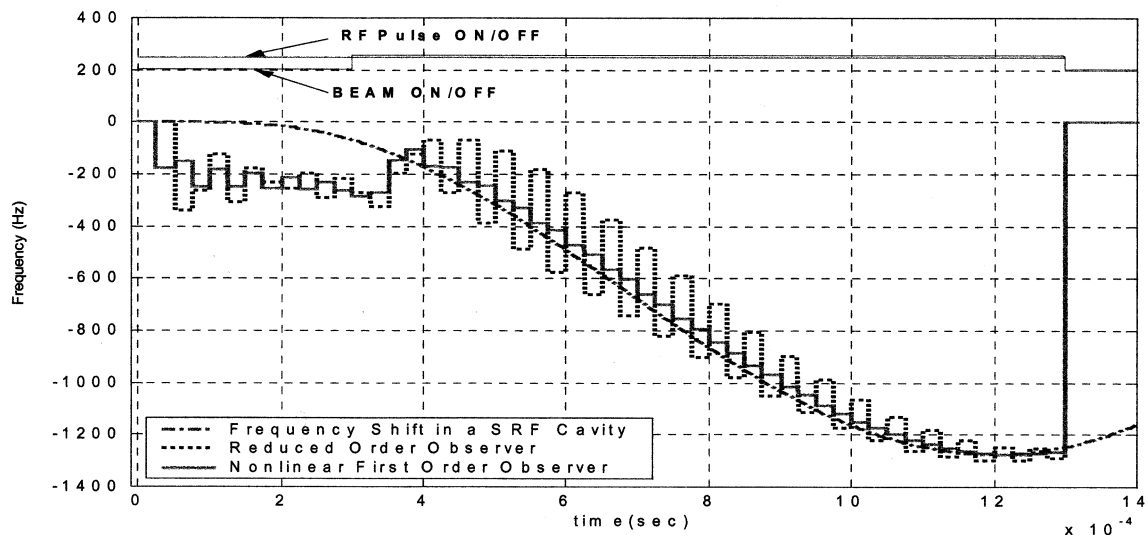


Fig. 5. Observer performances for the Lorentz force detuning in [3]. For the reduced observer, $r_1 = r_2 = 7.5398e4$ are used and for the nonlinear first-order observer, $l = 7.5398e4$ is used. Microphonics is not included in the model.

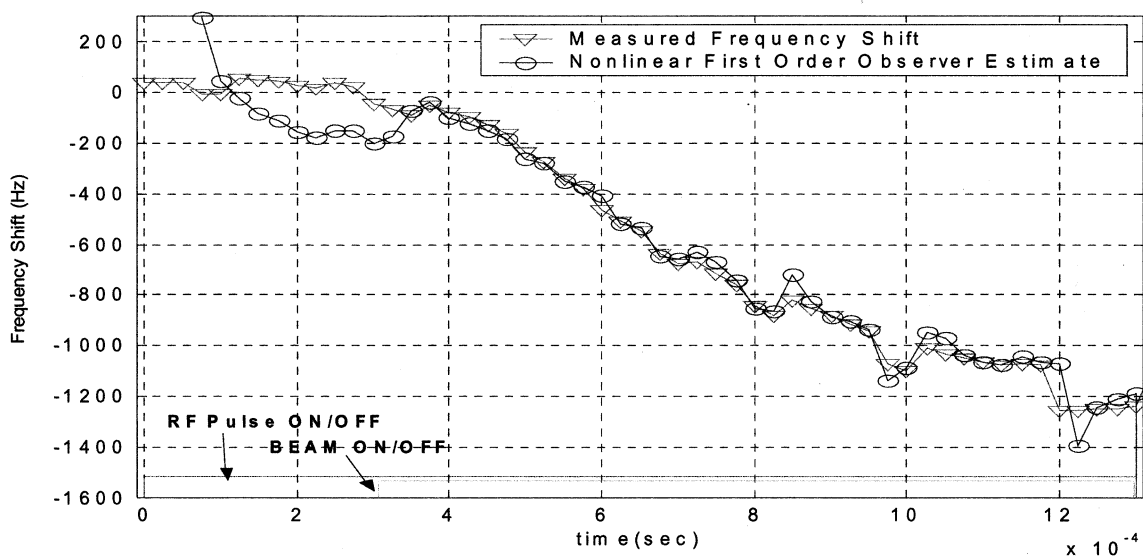


Fig. 6. DSP implementation result for nonlinear first-order observer performance experiment for the Lorentz force detuning in [3]. For the nonlinear first-order observer, $l = 6.2834e4$ is used. Microphonics is included in the model. The RF pulse ON period is 1.3 ms and the sampling frequency is 40 kHz. Hence, the total data points during one RF pulse are 52.

for the DSP, the computational time is $0.11 \mu\text{s}$. Hence, the sampling frequency should be less than 9.5 MHz. With this sampling frequency, observer gains can be determined so as to guarantee fast response of observers.

Numerical analysis addressed in [10] shows that the distribution of mechanical mode frequencies is up to a few thousand Hertz. However, the dominant mechanical mode vibrations which contribute to the Lorentz force detuning result from the several low frequencies. Hence, the proposed deterministic observers can be applied to estimate the Lorentz force detuning. Additionally, the frequencies of microphonics reported in [6] are less than a few hundred Hertz. Hence, the proposed observers

can be applied to estimate microphonics when it is deterministic. However, when microphonics is driven by stochastic noise processes, the deterministic frequency shift can be estimated by applying Kalman estimation technique [18].

VI. CONCLUSION

In this paper, three deterministic disturbance observers have been proposed to estimate the frequency shift in a SRF cavity. Through computer simulations, the performances of the observers were investigated and the appropriate observer for the real time implementation in a DSP was chosen. The

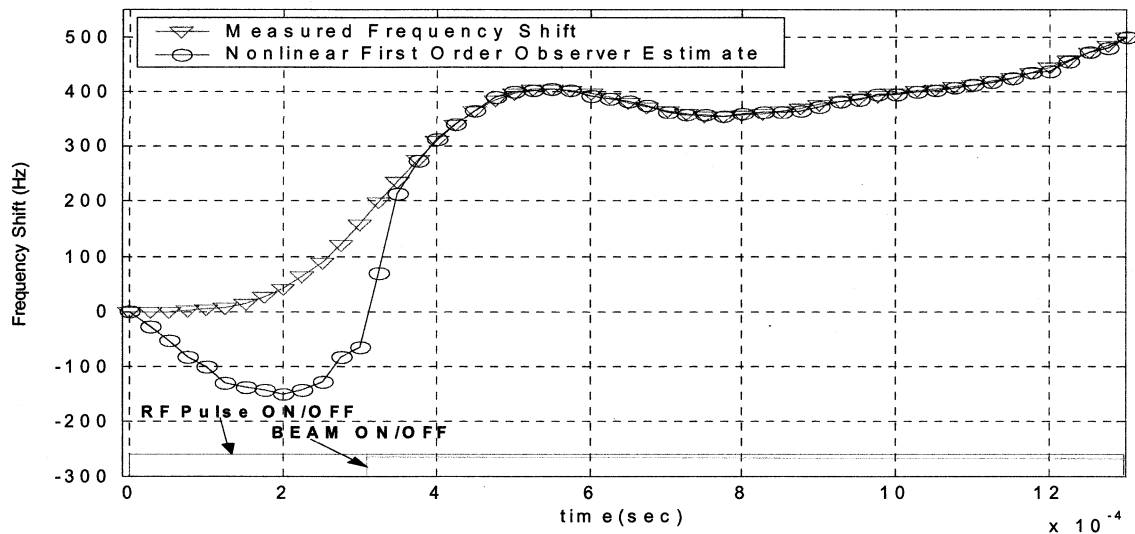


Fig. 7. DSP implementation result for nonlinear first-order observer performance experiment for the Lorentz force detuning in [8]. For the nonlinear first-order observer, $l = 6.2834e4$ is used. Microphonics is not included in the model. The RF pulse ON period is 1.3 ms and the sampling frequency is 40 kHz. Hence, the total data points during one RF pulse are 52.

selected observer, nonlinear first-order observer, is simple and yields the satisfactory performance. The observer algorithm was implemented in TMS320C6201 EVM and the observer performance was investigated. The experiment shows that the proposed observer had reasonable computational time and was reliable, promising for frequency shift estimation of a SRF cavity.

REFERENCES

- [1] T. Schilcher, "Vector Sum Control of Pulsed Accelerating Fields in Lorentz Force Detuned Superconducting Cavities," TESLA 98-20, DESY Rep., 1998.
- [2] H. Padamsee, J. Knobloch, and T. Hays, *RF Superconductivity for Accelerators*. New York: Wiley, 1998.
- [3] S.-I. Kwon, "Modeling of SNS SRF Control System and Power Control Margin Analysis," Los Alamos National Lab. SNS Document, no. SNS01_DES_0573, 2000. Final Design Review: SNS Super Conducting Linac RF Control System.
- [4] R. Sundelin, Update on medium- β K -requirements, , Jefferson Lab., Newport News, VA, 2001. preprint.
- [5] "SNS Parameters List," Los Alamos National Lab. SNS Document, Los Alamos, NM, SNS01_PMP_0444, 2000.
- [6] M. Liepe, W. D. Moller, H. B. Peters, and S. N. Simrock, "Active control of Lorentz-detuning and microphonics," presented at the Workshop on Low Level RF Controls for Superconducting Linacs, Newport News, VA, 2001.
- [7] C. Tsukishima, K. Mukugi, Y. Kijima, T. Murai, N. Ouchi, E. Chishiro, J. Kusano, and M. Mizumoto, "Modeling of a super-conducting cavity de-tuned by the Lorentz pressure," in *Proc. 12th Symp. Accelerator Science and Technology*, Japan, 1999, pp. 328–330.
- [8] E. Chishiro, N. Ouchi, K. Hasegawa, M. Mizumoto, and S. Noguchi, "Study of RF control system for superconducting cavity," in *Proc. 12th Symp. Accelerator Science and Technology*, Japan, 1999, pp. 236–238.
- [9] A. Mosnier, "Dynamic Measurements of the Lorentz Forces on a MACSE Cavity," CE Saclay, France, Tech. Rep. DAPNIA-SEA-92-05, 1992.
- [10] S. Ellis, "SNS SRF time dependent cavity of resonance shift due to Lorentz force induced mechanical excitation," in *Proc. 2001 Particle Accelerator Conf.*, Chicago, IL, 2001.
- [11] R. Mitchell, "Lorentz force detuning analysis of the SNS accelerating cavities," in *Proc. 10th Workshop on RF Superconductivity*, Japan, Sept. 2001.
- [12] S.-I. Kwon, A. Regan, and Y.-M. Wang, "SNS superconducting RF cavity model-iterative learning control," *Nucl. Instrum. Methods Phys. Rev. A*, vol. 482, pp. 12–31, 2002.
- [13] A. Isidori, *Nonlinear Control Systems*. London, U.K.: Springer-Verlag, 1995.
- [14] M. J. Kurtz and M. A. Henson, "State and disturbance estimation for nonlinear systems affine in the unmeasured variables," *Comput. Chem. Eng.*, vol. 22, no. 100, pp. 1441–1459, 1998.
- [15] *SIMULINK: Dynamic System Simulation for MATLAB*, 1997. Mathworks, Inc.
- [16] *Texas Instruments, TMS320C6X Evaluation Module-Reference Guide*, 1998. SPRU269. Texas Instruments.
- [17] S.-I. Kwon and A. Regan, "Control System Analysis for the Perturbed Linear Accelerator RF System," LANL, Los Alamos, NM, Rep. LA-UR-02-2100, 2002.
- [18] I. R. Petersen and A. V. Savkin, *Robust Kalman Filtering for Signals and Systems with Large Uncertainties*. Boston, MA: Birkhäuser, 1999.